

OPTIMAL CONTROL OF A FRACTIONAL ORDER SEIR MATHEMATICAL MODEL FOR COVID-19 PANDEMIC

DRAMANE OUEDRAOGO^{1,*}, MOUSSA BARRO¹, DIENE NGOM², ABOUDRAMANE GUIRO¹

¹Department of Mathematics, Universite Nazi BONI, Burkina Faso

²Department of Mathematics, Universite Assane Seck de Ziguinchor, Senegal

*Corresponding author: dramaneouedraogo268@yahoo.ca

Received Nov. 21, 2024

ABSTRACT. COVID-19 has put a significant responsibility on all of us around from its detection and its remediation. The globe suffer from lock down due to COVID-19 pandemic. The researchers are doing their best to discover the nature of this pandemic and try to produce the possible plans to control it. One of the most effective method to understand and control the evolution of this pandemic is to model it via an efficient mathematical model. In this paper, we propose to model the COVID-19 by fractional order SEIR model. We determine the basic reproduction number. The existence of a stable solution of the fractional order SEIR model is proved and the fractional order necessary conditions of four proposed control strategies are produced. The sensitivity of the fractional order COVID-19 SEIR model to the fractional order and the infection rate parameters are displayed. All studies are numerically simulated using PYTHON software via fractional order differential equation solver.

2020 Mathematics Subject Classification. 34E05, 34D05, 65L20..

Key words and phrases. COVID-19, corona virus disease, optimal control, reported and unreported cases, epidemic mathematical model.

1. INTRODUCTION

All the world states' governments introduce a big effort and vital measures to eliminate the outbreak of COVID-19 [16]. COVID-19 is a new progeny of coronavirus, SARS-CoV-2 and firstly detected in Wuhan, China [35]. In the few months after discovering it, the number of patients were increasing exponentially. The taken measures against COVID-19 until the day of writing these words didn't prevent the growth of infected cases around the globe. The World Health Organization situation report published in 25 May 2020 informed that 5304772 cases as total cases and 342029 deaths around the globe [33].

DOI: [10.28924/APJM/12-25](https://doi.org/10.28924/APJM/12-25)

Using mathematical model to predict the epidemics is very useful in order to understand the nature of the epidemic and to design an efficient strategies to control it [4, 14]. It is common to study the humanitarian diffusion of epidemics via SIR or SEIR models [11, 13]. Various models have been proposed to model and study COVID-19 pandemic. Taking into account the risk understanding and the accumulative issue of cases, COVID-19 pandemic has been modeled by Lin et al. via extending SEIR model [23] where S signifies the susceptible, E signifies the exposed, I signifies the infected and R signifies the removed cases.

In [3], Anastassopoulou et al. have suggested the SIR model in the discrete time mode taking into account the dead cases. In [7] by Casella, SIR model is expanded to study the delays effect and to compare the policies of containment. In [34] by Wu et al., the COVID-19 severity has been estimated using the dynamics of transition. In [12], the general multi-group SEIRA model was represented and numerically tested for modelling the diffusion of COVID-19 between a non-homogeneous population. The basic mathematical tool used to model several epidemics is differential equations in various modes (ordinary, fractional, with delay, randomly detected or partial) [20, 21]. Many research efforts have been widely done to control the outbreaks of epidemics via optimal control [15, 30]. The optimal control idea is to look for the utmost powerful plan that decreases the rate of infection to a possible minimum limit with optimal minimum cost of circulating a treatment or preventative inoculation [25, 29, 30]. These plans may include treatments, inoculation with vaccines, social distances, educational programs [5, 8]. The literature has several studies to control for example models of HIV [19], dengue fever [2], tuberculosis [28], delayed SIR [1] and delayed SIRS [21]. The fractional order differential equations add an extra dimensions in the study of dynamics of epidemiological models. Therefore the fractional version of many epidemical models have been investigated as in [25], [8] and [32].

Here, a new epidemiological fractional mathematical model for the COVID-19 epidemic is proposed as an extension of the classical SIR model, similar to that introduced by Gumel et al. for SARS in [18].

In this work, we consider the fractional order SEIR model and then we derive the fractional order necessary conditions for existence of a stable solution. In addition, we study an optimal control plans for the fractional order SEIR model via two control strategies that include the availability of vaccination and existence of treatments for the infected detected three population fraction phases. Applying the fractional order differential equations numerical solver using PYTHON software, we show the dynamics of the state variables of the model and display the effect of changing the fractional derivative order on the system response. Also, the effect of changing the infection rates on the fractional order SEIR model's state 3 variables. We also implement the optimal control strategies numerically for the fractional order SEIR model.

The remaining parts of the paper are organized as follows. In Section 2, Preliminaries and basic definition of the fractional derivative are introduced. Describing COVID-19 epidemic SEIR fractional

mathematical model is introduced in Section 3. The basic reproduction number is given in section 4. The details of the optimal control strategy and its implementation are given in Section 5. Numerical simulations of the uncontrolled fractional order SEIR model, the effects of changing the fractional derivative order on the system response and the effects of changing the infection rates are all given and numerical simulations of the controlled fractional order SEIR model and the effects of applying the proposed control strategies are represented in Section 6. The concluding remarks are put in Section 7 followed by the list of cited references.

2. PRELIMINARIES

In this subsection, some definitions and results are introduced firstly.

Definition 2.1. [36] A gamma function $\Gamma :]0; +\infty[\rightarrow \mathbb{R}$ is defined by

$$\Gamma(\alpha) = \int_0^{\infty} x^{\alpha-1} e^{-x} dx.$$

Definition 2.2. [36] For any $t > t_0$, the time Caputo fractional derivative of order α ($n < \alpha < n + 1$) with the lower limit $t_0 \geq 0$ for a function is defined by

$$\Delta^\alpha f(t) = \frac{d^\alpha f(t)}{dt^\alpha} = \frac{1}{\Gamma(n - \alpha)} \int_{t_0}^t \frac{f^{(n)}(s)}{(t - s)^{\alpha-n+1}} ds,$$

where $\Gamma(\cdot)$ is the Gamma function.

Remark 2.1. When $\alpha = n$,

$$\Delta^\alpha f(t) = f^{(n)}(t).$$

Definition 2.3. [22] A constant x^* is an equilibrium point of the Caputo fractional dynamical system:

$$\Delta^\alpha x(t) = f(t, x), \quad x(t_0) \geq 0,$$

if and only if $f(t, x^*) = 0$.

Lemma 2.1. [24] Consider the fractional-order system:

$$\Delta^\alpha x(t) = f(t, x), \quad t_0 \geq 0,$$

with the initial condition $x(t_0) = x_0$, where $\alpha \in (0, 1]$ and $f : [t_0, \infty) \times \Omega \rightarrow \mathbb{R}^n$, $\Gamma \in \mathbb{R}^n$, if $f(t, x)$ satisfies the local Lipschitz condition with respect to x , there exists a unique solution of the above system.

3. MODEL FORMULATION AND BASIC PROPERTIES

The following diagram shows the dynamic of the covid-19

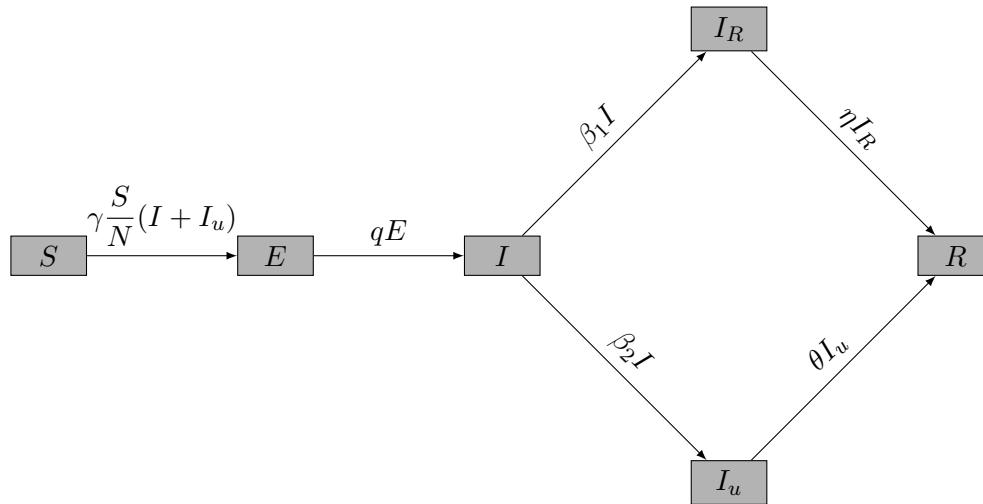


FIGURE 1. The compartmental diagram for the SEIR model

Then, according to Figure 1, we obtain the following system of six differential equations:

$$\left\{ \begin{array}{l} \Delta^\alpha S = -\gamma \frac{S}{N} (I + I_u), \\ \Delta^\alpha E = \gamma \frac{S}{N} (I + I_u) - qE, \\ \Delta^\alpha I = qE - \beta I, \\ \Delta^\alpha I_R = \beta_1 I - \eta I_R, \\ \Delta^\alpha I_u = \beta_2 I - \theta I_u, \\ \Delta^\alpha R = \eta I_R + \theta I_u, \end{array} \right. \quad (3.1)$$

where $S(t)$ is the number of individuals susceptible to infection at time t , $E(t)$ is the number of individuals exposed at time t , $I(t)$ is the number of asymptomatic infectious individuals at time t , $I_R(t)$ is the number of reported symptomatic infectious individuals (i.e symptomatic infectious with sever symptoms) at time t , and $I_u(t)$ is the number of unreported symptomatic infectious individuals (i.e., symptomatic infectious with mild symptoms) at time t , $R(t)$ is recovered individuals at times t . The

initial conditions $S(0), E(0), I(0), I_R(0), I_u(0)$ and $S(0)$ are all positive.

Since summing up all equations of (3.1) gives zero as a result then the system is compartmentalized and shows the conservation property of mass : as can be directly proved,

$$\Delta^\alpha S + \Delta^\alpha E + \Delta^\alpha I + \Delta^\alpha I_R + \Delta^\alpha I_u + \Delta^\alpha R = 0.$$

Which implies that the total population (the sum of all state variables) is constant.

The parameters are positive and defined as follows:

Parameter	Definition
γ	Transmission rate
q	Rate that exposed individuals become infectious
β	Rate that exposed individuals become unreported or reported infectious individuals
β_1	Rate that unreported individuals
β_2	Rate that reported individuals
η	Rate that reported individuals become Recovered
θ	Rate that unreported individuals become Recovered

Proposition 3.1. *The basic reproduction number for model system (3.1) is defined by*

$$R_0 = \frac{\gamma S^0}{\beta N} \left(1 + \frac{\beta_2}{\theta} \right),$$

where the disease-free equilibrium for system (3.1) is given by $E_0 = (S^0, 0, 0, 0, 0)$ with $S^0 = N$.

Proof. We use the method in [31] to compute the reproduction number R_0 .

We get

$$\mathcal{F} = \begin{pmatrix} \mathcal{F}_1 \\ \mathcal{F}_2 \\ \mathcal{F}_3 \\ \mathcal{F}_4 \end{pmatrix} = \begin{pmatrix} \gamma \frac{S}{N} (I + I_u) \\ 0 \\ 0 \\ 0 \end{pmatrix} \text{ and } \mathcal{V} = \begin{pmatrix} \mathcal{V}_1 \\ \mathcal{V}_2 \\ \mathcal{V}_3 \\ \mathcal{V}_4 \end{pmatrix} = \begin{pmatrix} -qE \\ qE - \beta I \\ \beta_1 I - \eta I_R \\ \beta_2 I - \theta I_u \end{pmatrix}, \quad (3.2)$$

We have

$$\mathcal{DF} = \begin{pmatrix} \frac{\partial \mathcal{F}_1}{\partial E} & \frac{\partial \mathcal{F}_1}{\partial I} & \frac{\partial \mathcal{F}_1}{\partial I_R} & \frac{\partial \mathcal{F}_1}{\partial I_u} \\ \frac{\partial \mathcal{F}_2}{\partial E} & \frac{\partial \mathcal{F}_2}{\partial I} & \frac{\partial \mathcal{F}_2}{\partial I_R} & \frac{\partial \mathcal{F}_2}{\partial I_u} \\ \frac{\partial \mathcal{F}_3}{\partial E} & \frac{\partial \mathcal{F}_3}{\partial I} & \frac{\partial \mathcal{F}_3}{\partial I_R} & \frac{\partial \mathcal{F}_3}{\partial I_u} \\ \frac{\partial \mathcal{F}_4}{\partial E} & \frac{\partial \mathcal{F}_4}{\partial I} & \frac{\partial \mathcal{F}_4}{\partial I_R} & \frac{\partial \mathcal{F}_4}{\partial I_u} \end{pmatrix} = \begin{pmatrix} 0 & \gamma \frac{S}{N} & 0 & \gamma \frac{S}{N} \\ 0 & 0 & 0 & 0 \\ 0 & 0 & 0 & 0 \\ 0 & 0 & 0 & 0 \end{pmatrix} \quad (3.3)$$

and

$$D\mathcal{V} = \begin{pmatrix} \frac{\partial \mathcal{V}_1}{\partial E} & \frac{\partial \mathcal{V}_1}{\partial I} & \frac{\partial \mathcal{V}_1}{\partial I_R} & \frac{\partial \mathcal{V}_1}{\partial I_u} \\ \frac{\partial \mathcal{V}_2}{\partial E} & \frac{\partial \mathcal{V}_2}{\partial I} & \frac{\partial \mathcal{V}_2}{\partial I_R} & \frac{\partial \mathcal{V}_2}{\partial I_u} \\ \frac{\partial \mathcal{V}_3}{\partial E} & \frac{\partial \mathcal{V}_3}{\partial I} & \frac{\partial \mathcal{V}_3}{\partial I_R} & \frac{\partial \mathcal{V}_3}{\partial I_u} \\ \frac{\partial \mathcal{V}_4}{\partial E} & \frac{\partial \mathcal{V}_4}{\partial I} & \frac{\partial \mathcal{V}_4}{\partial I_R} & \frac{\partial \mathcal{V}_4}{\partial I_u} \end{pmatrix} = \begin{pmatrix} -\alpha & 0 & 0 & 0 \\ \alpha & -\beta & 0 & 0 \\ 0 & \beta_1 & -\eta & 0 \\ 0 & \beta_2 & 0 & -\theta \end{pmatrix}. \quad (3.4)$$

On $E_0 = (S^0, 0, 0, 0)$, we get

$$F = \begin{pmatrix} 0 & \gamma \frac{S^0}{N} & 0 & \gamma \frac{S^0}{N} \\ 0 & 0 & 0 & 0 \\ 0 & 0 & 0 & 0 \\ 0 & 0 & 0 & 0 \end{pmatrix} \quad (3.5)$$

and

$$V = \begin{pmatrix} -\alpha & 0 & 0 & 0 \\ \alpha & -\beta & 0 & 0 \\ 0 & \beta_1 & -\eta & 0 \\ 0 & \beta_2 & 0 & -\theta \end{pmatrix}, \quad (3.6)$$

Thus, we obtain

$$-FV^{-1} = \begin{pmatrix} \frac{\gamma S^0}{\beta N} + \frac{\gamma S^0 \beta_2}{\theta \beta N} & \frac{\gamma S^0}{\beta N} - \frac{\gamma S^0 \beta_2}{\theta \beta N} & 0 & \frac{\gamma S^0}{\theta N} \\ 0 & 0 & 0 & 0 \\ 0 & 0 & 0 & 0 \\ 0 & 0 & 0 & 0 \end{pmatrix}, \quad (3.7)$$

The basic reproduction number is defined as the dominant eigenvalue of the matrix $-FV^{-1}$.

Therefore,

$$R_0 = \frac{\gamma S^0}{\beta N} \left(1 + \frac{\beta_2}{\theta} \right). \quad (3.8)$$

Remark 3.1. The basic reproduction number evaluate the average number of new infections generated by a single infected individual in a completely susceptible population.

4. FRACTION ORDER SEIR MODEL'S OPTIMAL CONTROL STRATEGY

In this section, the existence of the fractional order SEIR model's optimal control is investigated and then the Hamiltonian of the optimal control problem is constructed in order to produce the optimal control necessary requirements.

Compute the optimal values of vaccination u_1 and treatment strategies u_2 that would maximize the recovered individuals R and minimize the number of reported symptomatic infectious individuals $I_R(t)$. In addition, the charges of utilizing the vaccination and treatment methods are minimized. Then the optimal control problem of the following form is considered (see for example [6])

$$\min_{(u_1, u_2) \in \mathbb{U}} J(u_1(t), u_2(t)) = S(T) + I_R(T) - R(T) + \int_0^T (c_1 u_1^2(t) + c_2 u_2^2(t) + S(t) + I_R(t) - R(t)) dt \quad (4.1)$$

subject to the state equation

$$\left\{ \begin{array}{l} \Delta^\alpha S = -\gamma \frac{S}{N}(I + I_u) - u_1 S, \\ \Delta^\alpha E = \gamma \frac{S}{N}(I + I_u) - qE, \\ \Delta^\alpha I = qE - \beta I, \\ \Delta^\alpha I_R = \beta_1 I - \eta I_R - u_2 I_R, \\ \Delta^\alpha I_u = \beta_2 I - \theta I_u, \\ \Delta^\alpha R = (u_2 + \eta) I_R + \theta I_u + u_1 S, \end{array} \right. \quad (4.2)$$

The two functions u_1 and u_2 represent vaccination and treatment strategies. These control functions are assumed to be $L^\infty(0, T)$ functions belonging to a set of admissible controls

$$\mathbb{U} = \{(u_1, u_2) \in L^\infty(0, T) \times L^\infty(0, T) : u_{1min} \leq u_1(t) \leq u_{1max}, u_{2min} \leq u_2(t) \leq u_{2max}\},$$

where $0 \leq u_{1min} < u_{1max} \leq 1$ and $0 \leq u_{2min} < u_{2max} \leq 1$. The two constants c_1 and c_2 are weighted cost associated with the use of the controls $u_1(t)$ and $u_2(t)$, respectively.

4.1. Existence of optimal control. To show the existence of the optimal control for the problem under consideration, we notice that the set of admissible controls \mathbb{U} is, by definition, closed and bounded. It is also convex because $[u_{1min}, u_{1max}] \times [u_{2min}, u_{2max}]$ is convex in \mathbb{R}^2 . It is obvious that there is an admissible pair $((u_1(t), u_2(t)), (S(t), E(t), I(t), I_R(t), I_u(t), R(t)))$ for the problem. Hence, the existence

of the optimal control comes as a direct result from the Filippove-Cesari theorem [26]. We therefore, have the following result.

Theorem 4.1. *Consider the optimal control problem (4.1) subject to (4.2). Then there exists an optimal pair of controls (u_1^*, u_2^*) and a corresponding optimal states $(S^*, E^*, I^*, I_R^*, I_u^*, R^*)$ that minimizes the objective function J over set of admissible controls \mathbb{U} .*

proof. To prove the existence of an optimal control pair, it is important to verify the following facts:

- (1) The set of controls and corresponding state variables is nonempty,
- (2) The admissible set \mathbb{U} is convex and closed,
- (3) The right-hand side of the state system (4.2) is bounded by a linear function in the state and control variables,
- (4) The integrand of the objective functional is convex on \mathbb{U} ,
- (5) There exists constants $\omega_1, \omega_2 > 0$, and $\rho > 1$ such that the integrand $L(S, I_R, R, u_1, u_2)$ of the objective functional satisfies $L(S, I_R, R, u_1, u_2) \geq \omega_2 + \omega_1|(u_1, u_2)|^\rho$.

4.2. Characterization of optimal control. In this subsection, we derive the first order necessary conditions for the existence of optimal control, by constructing the Hamiltonian H and applying the Pontryagin's maximum principle.

To simplify the notations, we write $x(t) = [S(t), E(t), I(t), I_R(t), I_u(t), R(t)]^T$, $u(t) = [u_1(t), u_2(t)]^T$ and $\lambda(t) = [\lambda_1(t), \lambda_2(t), \lambda_3(t), \lambda_4(t), \lambda_5(t), \lambda_6(t)]$. We denote by $g(u(t), x(t))$ the integrand part of the objective function (4.1). With these notations and terminologies, the Hamiltonian is given by

$$\begin{aligned}
 H(u, x, \lambda) &= g(u, x) + \lambda^T \cdot \dot{x} \\
 &= c_1 u_1^2 + c_2 u_2^2 + S + I_R - R + \lambda_1 \left(-\gamma \frac{S}{N} (I + I_u) - u_1 S \right) \\
 &\quad + \lambda_2 \left(\gamma \frac{S}{N} (I + I_u) - qE \right) + \lambda_3 \left(qE - \beta I \right) + \lambda_4 \left(\beta_1 I - \eta I_R - u_2 I_R \right) \\
 &\quad + \lambda_5 \left(\beta_2 I - \theta I_u \right) + \lambda_6 \left(u_2 I_R + \eta I_R + \theta I_u + u_1 S \right)
 \end{aligned} \tag{4.3}$$

Let $u^* = [u_1^*, u_2^*]^T$ be the optimal control and $x^*(t) = [S^*(t), E^*(t), I^*(t), I_R^*(t), I_u^*(t), R^*(t)]^T$ be the corresponding optimal trajectory. Then there exists $\lambda(t) \in \mathbb{R}^6$ such that the first order necessary conditions for the existence of optimal control are given by the equations

$$\frac{\partial H}{\partial u}(t) = 0, \tag{4.4}$$

$$\Delta^\alpha x(t) = \frac{\partial H}{\partial \lambda}, \tag{4.5}$$

$$\Delta^\alpha \lambda(t) = -\frac{\partial H}{\partial x} \tag{4.6}$$

The optimality conditions:

$$\left[\frac{\partial H}{\partial u_1}(t) \right]_{u_1(t)=u_1^*(t)} = 0 \quad (4.7)$$

$$\left[\frac{\partial H}{\partial u_2}(t) \right]_{u_2(t)=u_2^*(t)} = 0 \quad (4.8)$$

Simplifying (4.7) and (4.8) we obtain

$$2c_1 u_1^* - \lambda_1 S + \lambda_6 S = 0 \quad (4.9)$$

$$2c_2 u_2^* - \lambda_4 I_R + \lambda_6 I_R = 0 \quad (4.10)$$

Further simplification of (4.9) and (4.10) yields

$$u_1^*(t) = \min \left\{ u_{1max}; \max \left\{ 0; \frac{(\lambda_1(t) - \lambda_6(t))S(t)}{2c_1} \right\} \right\} \quad (4.11)$$

and

$$u_2^*(t) = \min \left\{ u_{2max}; \max \left\{ 0; \frac{(\lambda_4(t) - \lambda_6(t))I_R(t)}{2c_2} \right\} \right\} \quad (4.12)$$

The state equations: given by the forms (4.2)

The co-state equations which when simplified, lead to

$$\Delta^\alpha \lambda_1(t) = -\frac{\partial H}{\partial S} = -1 + \lambda_1 \left(\gamma \frac{1}{N} (I + I_u) - u_1 \right) - \lambda_2 \left(\gamma \frac{1}{N} (I + I_u) \right) - \lambda_6 u_1; \quad (4.13)$$

$$\Delta^\alpha \lambda_2(t) = -\frac{\partial H}{\partial E} = q(\lambda_2 - \lambda_3); \quad (4.14)$$

$$\Delta^\alpha \lambda_3(t) = -\frac{\partial H}{\partial I} = \gamma \frac{S}{N} (\lambda_1 - \lambda_2) + \lambda_3 \beta - \lambda_4 \beta_1 - \lambda_5 \beta_2 \quad (4.15)$$

$$\Delta^\alpha \lambda_4(t) = -\frac{\partial H}{\partial I_R} = -1 + \eta(\lambda_4 - \lambda_6) + u_2(\lambda_4 - \lambda_6); \quad (4.16)$$

$$\Delta^\alpha \lambda_5(t) = -\frac{\partial H}{\partial I_u} = \gamma \frac{S}{N} (\lambda_1 - \lambda_2) + \theta(\lambda_5 - \lambda_6); \quad (4.17)$$

$$\Delta^\alpha \lambda_6(t) = -\frac{\partial H}{\partial R} = 1 \quad (4.18)$$

The transversality conditions:

$$\lambda_1(T) = 1; \quad (4.19)$$

$$\lambda_2(T) = 0; \quad (4.20)$$

$$\lambda_3(T) = 1; \quad (4.21)$$

$$\lambda_4(T) = 0; \quad (4.22)$$

$$\lambda_5(T) = 0; \quad (4.23)$$

$$\lambda_6(T) = -1. \quad (4.24)$$

The effect of applying the different control strategies will be simulated numerically in Section 5

5. FRACTION ORDER NUMERICAL SIMULATION OF THE SEIR UNCONTROLLED MODEL

In this section, we solve the fractional order *SEIR* model numerically utilising the discretization in [27]. The parameters' values used for the numerical simulation was published by Guiro et al. in [17] where: $q = 0.1818$, $\eta = \theta = \frac{1}{14}$, $\beta = \frac{1}{7}$, $\beta_1 = 0.1$, $\beta_2 = 0.0428$, $\gamma = 0.7$ and the initial values of the different population are $S(0) = 20000000$, $E(0) = 200$, $I(0) = 0$, $I_u(0) = 0$, $I_R(0) = 0$, $R(0) = 0$. In the following, we display the results of the numerical simulation of the uncontrolled *SEIR* model.

Figure 2 shows the evolution of susceptible cases ($S(t)$) with different fractional derivative order (α).

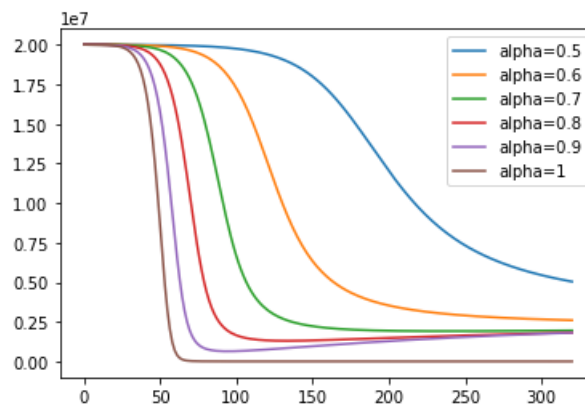


FIGURE 2. The susceptible population S without controls for $\alpha = 0.5, 0.6, 0.7, 0.9, 1$.

Figure 3 represents the evolution of Exposed cases ($E(t)$) with different fractional derivative order (α).

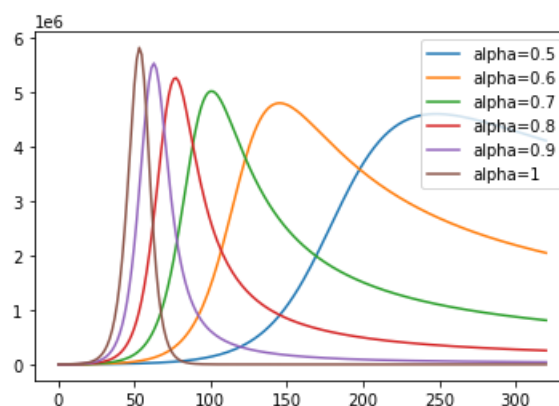


FIGURE 3. The exposed population E without controls for $\alpha = 0.5, 0.6, 0.7, 0.9, 1$.

Figure 4 represents the evolution of Infected cases ($I(t)$) with different fractional derivative order (α).

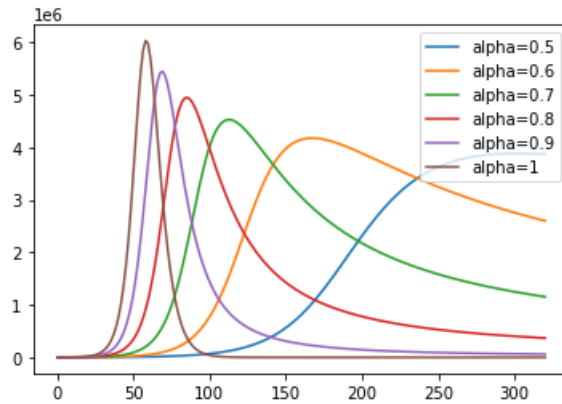


FIGURE 4. The infected population I without controls for $\alpha = 0.5, 0.6, 0.7, 0.9, 1$.

Figure 5 shows the evolution of reported Infected cases ($I_R(t)$) with different fractional derivative order (α).

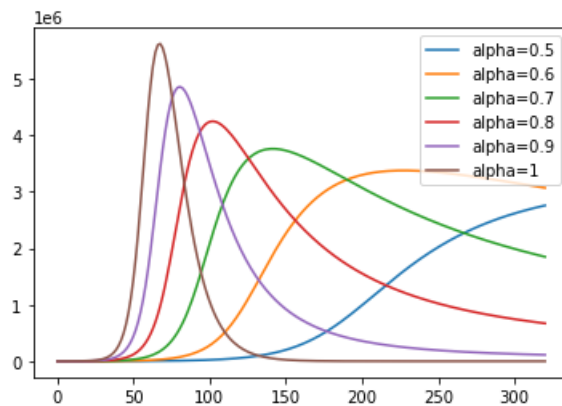


FIGURE 5. The reported infected population I_R without controls for $\alpha = 0.5, 0.6, 0.7, 0.9, 1$.

Figure 6 represents the evolution of unreported Infected cases ($I_u(t)$) with different fractional derivative order (α).

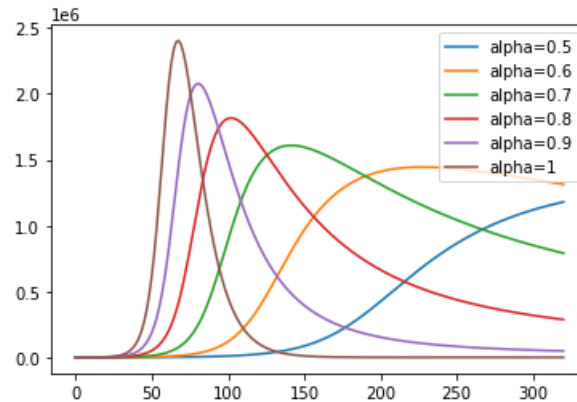


FIGURE 6. The unreported infected population I_u without controls for $\alpha = 0.5, 0.6, 0.7, 0.9, 1$.

Figure 7 represents the evolution of recovered cases ($R(t)$) with different fractional derivative order (α).

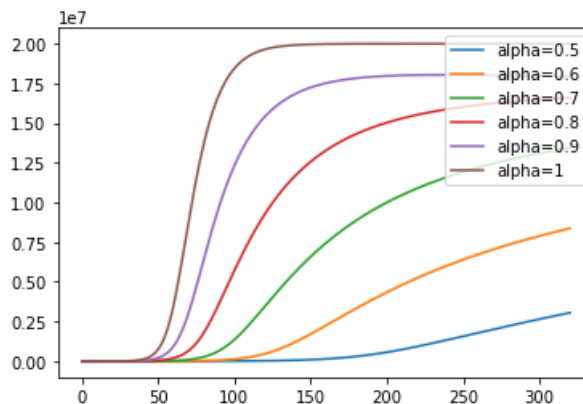


FIGURE 7. The recovered population R without controls for $\alpha = 0.5, 0.6, 0.7, 0.9, 1$.

From the results and the figures mentioned here, we can state that decreasing the fractional derivative order decreases the number of each population phase (except Susceptible population fraction as expected) and flatten the curves also delays reaching the maximum in each population phase.

6. NUMERICAL SIMULATION OF THE CONTROLLED SYSTEM

In this section, we show numerically, the effect of applying the two control strategies studied in Section 4.

Figure 8 shows the time history of Susceptible cases with control (vaccination and treatment are available) with different fractional derivative order: $\alpha = 0.5, 0.6, 0.7, 0.9, 1$.

Figure 9 shows the time history of Exposed cases with control (vaccination and treatment are available) with different fractional derivative order: $\alpha = 0.5, 0.6, 0.7, 0.9, 1$.

Figure 10 shows the time history of infected cases with control (vaccination and treatment are available) with different fractional derivative order: $\alpha = 0.5, 0.6, 0.7, 0.9, 1$.

Figure 11 shows the time history of reported infected cases with control (vaccination and treatment are available) with different fractional derivative order: $\alpha = 0.5, 0.6, 0.7, 0.9, 1$.

Figure 12 shows the time history of unreported infected cases with control (vaccination and treatment are available) with different fractional derivative order: $\alpha = 0.5, 0.6, 0.7, 0.9, 1$.

Figure 13 shows the time history of recovered cases with control (vaccination and treatment are available) with different fractional derivative order: $\alpha = 0.5, 0.6, 0.7, 0.9, 1$.

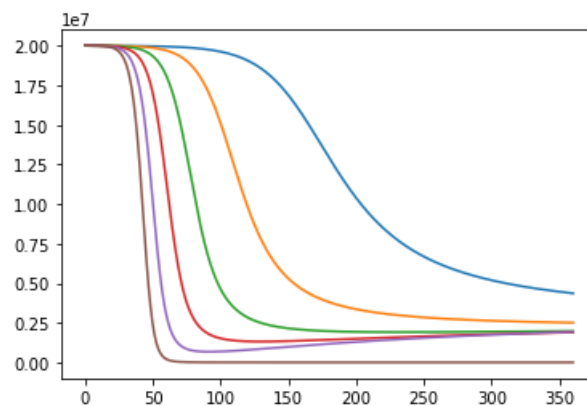


FIGURE 8. Time history of Susceptible cases with control (vaccination and treatment are available) with different fractional derivative order: $\alpha = 0.5, 0.6, 0.7, 0.9, 1$.

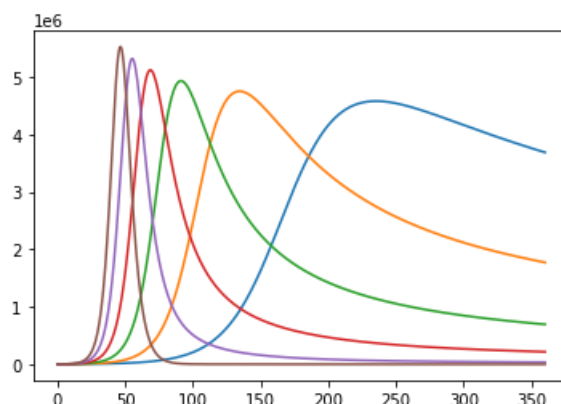


FIGURE 9. Time history of Exposed cases with control (vaccination and treatment are available) with different fractional derivative order: $\alpha = 0.5, 0.6, 0.7, 0.9, 1$.

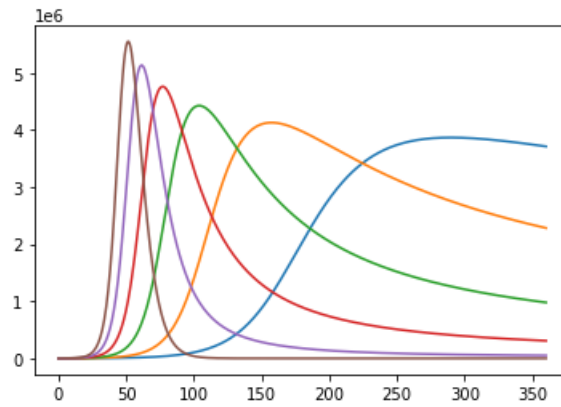


FIGURE 10. Time history of infected cases with control (vaccination and treatment are available) with different fractional derivative order: $\alpha = 0.5, 0.6, 0.7, 0.9, 1$.

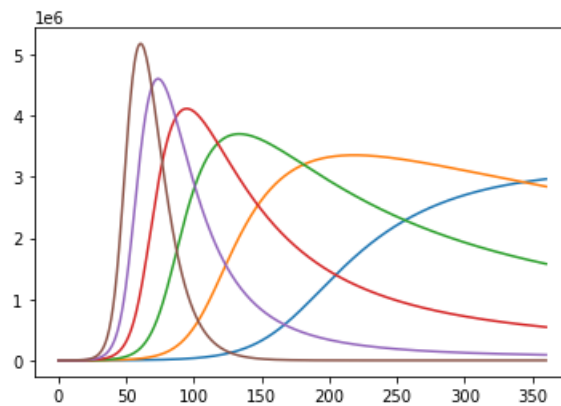


FIGURE 11. Time history of reported infected cases with control (vaccination and treatment are available) with different fractional derivative order: $\alpha = 0.5, 0.6, 0.7, 0.9, 1$.

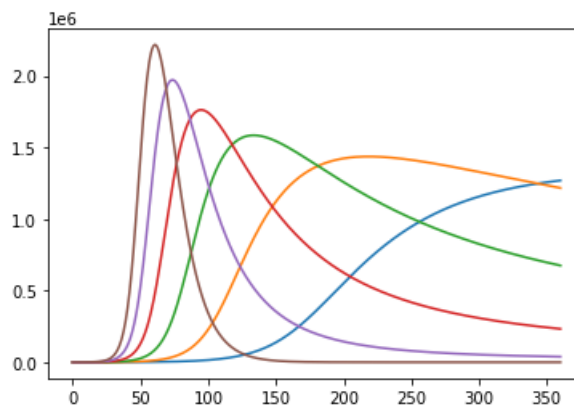


FIGURE 12. Time history of unreported infected cases with control (vaccination and treatment are available) with different fractional derivative order: $\alpha = 0.5, 0.6, 0.7, 0.9, 1$.

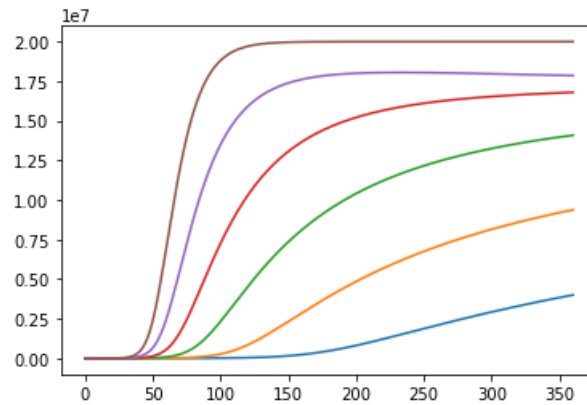


FIGURE 13. Time history of recovered cases with control (vaccination and treatment are available) with different fractional derivative order: $\alpha = 0.5, 0.6, 0.7, 0.9, 1$.

7. CONCLUSION

This research has been carried out to the analysis of an six dimension fractional-order SEIR COVID-19 mathematical model. In this study of COVID-19 mathematical model, the infected population fraction is partitioned into two different population fractions: I_R et I_u . The fractional-order necessary conditions for a two optimal control strategies are implemented. In addition, the system dynamics displayed via the fraction order numerical solver by PYTHON software with different fractional orders are presented in this manuscript. The dynamics of the system are presented before control. From our study, we can state that decreasing the fractional derivative order decreases the number of cases in all population fraction phases and delays the maximum. The fractional order COVID-19 SEIR model predicts the evolution of COVID-19 epidemic and try to help in understanding the impact of different plans to limit the diffusion of this epidemic with different values of the fractional order.

Authors' Contributions. All authors have read and approved the final version of the manuscript. The authors contributed equally to this work.

Conflicts of Interest. The authors declare that there are no conflicts of interest regarding the publication of this paper.

REFERENCES

- [1] A. Abta, H. Laarabi, H. Talibi Alaoui, The Hopf Bifurcation Analysis and Optimal Control of a Delayed SIR Epidemic Model, *Int. J. Anal.* 2014 (2014), 940819. <https://doi.org/10.1155/2014/940819>.
- [2] D. Aldila, T. Götz, E. Soewono, An Optimal Control Problem Arising from a Dengue Disease Transmission Model, *Math. Biosci.* 242 (2013), 9–16. <https://doi.org/10.1016/j.mbs.2012.11.014>.
- [3] C. Anastassopoulou, L. Russo, A. Tsakris, C. Siettos, Data-Based Analysis, Modelling and Forecasting of the COVID-19 Outbreak, *PLOS ONE* 15 (2020), e0230405. <https://doi.org/10.1371/journal.pone.0230405>.

- [4] R.M. Anderson, R.M. May, *Infectious Diseases of Humans: Dynamics and Control*, Oxford University Press, Oxford, 1991. <https://doi.org/10.1093/oso/9780198545996.001.0001>.
- [5] F.G. Ball, E.S. Knock, P.D. O'Neill, Control of Emerging Infectious Diseases Using Responsive Imperfect Vaccination and Isolation, *Math. Biosci.* 216 (2008), 100–113. <https://doi.org/10.1016/j.mbs.2008.08.008>.
- [6] M. Barro, A. Guiro, D. Ouedraogo, Optimal Control of a SIR Epidemic Model with General Incidence Function and a Time Delays, *Cubo (Temuco)* 20 (2018), 53–66. <https://doi.org/10.4067/S0719-06462018000200053>.
- [7] F. Casella, Can the COVID-19 Epidemic Be Controlled on the Basis of Daily Test Reports?, *IEEE Control Syst. Lett.* 5 (2021), 1079–1084. <https://doi.org/10.1109/LCSYS.2020.3009912>.
- [8] C. Castilho, Optimal Control of an Epidemic Through Educational Campaigns, *Electron. J. Differ. Equ.* 2006 (2006), 125.
- [9] C. Castillo-Chavez, A.A. Yakubu, Dispersal, Disease and Life-History Evolution, *Math. Biosci.* 173 (2001), 35–53. [https://doi.org/10.1016/S0025-5564\(01\)00065-7](https://doi.org/10.1016/S0025-5564(01)00065-7).
- [10] C. Castillo-Chavez, A.A. Yakubu, Discrete-Time S-I-S Models with Complex Dynamics, *Nonlinear Anal.: Theory Methods Appl.* 47 (2001), 4753–4762. [https://doi.org/10.1016/S0362-546X\(01\)00587-9](https://doi.org/10.1016/S0362-546X(01)00587-9).
- [11] C. Chiyaka, W. Garira, S. Dube, Transmission Model of Endemic Human Malaria in a Partially Immune Population, *Math. Comput. Model.* 46 (2007), 806–822. <https://doi.org/10.1016/j.mcm.2006.12.010>.
- [12] S. Contreras, H.A. Villavicencio, D. Medina-Ortiz, J.P. Biron-Lattes, Á. Olivera-Nappa, A Multi-Group SEIRA Model for the Spread of COVID-19 among Heterogeneous Populations, *Chaos Solitons Fractals* 136 (2020), 109925. <https://doi.org/10.1016/j.chaos.2020.109925>.
- [13] M.-F. Danca, N. Kuznetsov, Matlab Code for Lyapunov Exponents of Fractional-Order Systems, *Int. J. Bifurcat. Chaos* 28 (2018), 1850067. <https://doi.org/10.1142/S0218127418500670>.
- [14] A.W. Roddam, *Mathematical Epidemiology of Infectious Diseases: Model Building, Analysis and Interpretation*, *Int. J. Epidemiol.* 30 (2001), 186–186. <https://doi.org/10.1093/ije/30.1.186>.
- [15] H. Gaff, E. Schaefer, Optimal Control Applied to Vaccination and Treatmentstrategies for Various Epidemiological Models, *Math. Biosci. Eng.* 6 (2009), 469–492. <https://doi.org/10.3934/mbe.2009.6.469>.
- [16] W. Guan, Z. Ni, Y. Hu, et al. Clinical Characteristics of Coronavirus Disease 2019 in China, *N. Engl. J. Med.* 382 (2020), 1708–1720. <https://doi.org/10.1056/NEJMoa2002032>.
- [17] A. Guiro, B. Koné, S. Ouaro, Mathematical Model of the Spread of the Coronavirus Disease 2019 (COVID-19) in Burkina Faso, *Appl. Math.* 11 (2020), 1204–1218. <https://doi.org/10.4236/am.2020.1111082>.
- [18] A.B. Gumel, S. Ruan, T. Day, et al. Modelling Strategies for Controlling SARS Outbreaks, *Proc. R. Soc. Lond. Ser. B: Biol. Sci.* 271 (2004), 2223–2232. <https://doi.org/10.1098/rspb.2004.2800>.
- [19] K. Hattaf, N. Yousfi, Optimal Control of a Delayed HIV Infection Model with ImmuneResponse Using an Efficient Numerical Method, *ISRN Biomath.* 2012 (2012), 215124. <https://doi.org/10.5402/2012/215124>.
- [20] H.W. Hethcote, P. Van Den Driessche, Some Epidemiological Models with Nonlinear Incidence, *J. Math. Biol.* 29 (1991), 271–287. <https://doi.org/10.1007/BF00160539>.
- [21] A. Kaddar, On the Dynamics of a Delayed Sir Epidemic Model With a Modified Saturated Incidence Rate, *Electron. J. Differ. Equ.* 2009 (2009), 133.
- [22] Y. Li, Y. Chen, I. Podlubny, Stability of Fractional-Order Nonlinear Dynamic Systems: Lyapunov Direct Method and Generalized Mittag–Leffler Stability, *Comput. Math. Appl.* 59 (2010), 1810–1821. <https://doi.org/10.1016/j.camwa.2009.08.019>.

- [23] Q. Lin, S. Zhao, D. Gao, et al. A Conceptual Model for the Coronavirus Disease 2019 (COVID-19) Outbreak in Wuhan, China with Individual Reaction and Governmental Action, *Int. J. Infect. Dis.* 93 (2020), 211–216. <https://doi.org/10.1016/j.ijid.2020.02.058>.
- [24] Y. Liu, A.A. Gayle, A. Wilder-Smith, J. Rocklöv, The Reproductive Number of COVID-19 Is Higher Compared to SARS Coronavirus, *J. Travel Med.* 27 (2020), taaa021. <https://doi.org/10.1093/jtm/taaa021>.
- [25] A.M.S. Mahdy, N.H. Sweilam, M. Higazy, Approximate Solution for Solving Nonlinear Fractional Order Smoking Model, *Alex. Eng. J.* 59 (2020), 739–752. <https://doi.org/10.1016/j.aej.2020.01.049>.
- [26] S. Nababan, A Filippov-Type Lemma for Functions Involving Delays and Its Application to Time-Delayed Optimal Control Problems, *J. Optim. Theory Appl.* 27 (1979), 357–376. <https://doi.org/10.1007/BF00933030>.
- [27] S. Qureshi, A. Yusuf, Modeling Chickenpox Disease with Fractional Derivatives: From Caputo to Atangana-Baleanu, *Chaos Solitons Fractals* 122 (2019), 111–118. <https://doi.org/10.1016/j.chaos.2019.03.020>.
- [28] S. Ruan, D. Xiao, J.C. Beier, On the Delayed Ross–Macdonald Model for Malaria Transmission, *Bull. Math. Biol.* 70 (2008), 1098–1114. <https://doi.org/10.1007/s11538-007-9292-z>.
- [29] D. Torres, C. Silva, Optimal Control Strategies for Tuberculosis Treatment: A Case Study in Angola, *Numer. Algebra Control Optim.* 2 (2012), 601–617. <https://doi.org/10.3934/naco.2012.2.601>.
- [30] N.H. Sweilam, S.M. AL-Mekhlafi, Optimal Control for a Nonlinear Mathematical Model of Tumor under Immune Suppression: A Numerical Approach, *Optim. Control Appl. Methods* 39 (2018), 1581–1596. <https://doi.org/10.1002/oca.2427>.
- [31] P. Van Den Driessche, J. Watmough, Reproduction Numbers and Sub-Threshold Endemic Equilibria for Compartmental Models of Disease Transmission, *Math. Biosci.* 180 (2002), 29–48. [https://doi.org/10.1016/S0025-5564\(02\)00108-6](https://doi.org/10.1016/S0025-5564(02)00108-6).
- [32] W. Wang, M.A. Khan, Analysis and Numerical Simulation of Fractional Model of Bank Data with Fractal–Fractional Atangana–Baleanu Derivative, *J. Comput. Appl. Math.* 369 (2020), 112646. <https://doi.org/10.1016/j.cam.2019.112646>.
- [33] WHO, Coronavirus Disease 2019 (COVID-19): Situation Report 126, World Health Organization, 2020.
- [34] J.T. Wu, K. Leung, M. Bushman, et al. Estimating Clinical Severity of COVID-19 from the Transmission Dynamics in Wuhan, China, *Nat. Med.* 26 (2020), 506–510. <https://doi.org/10.1038/s41591-020-0822-7>.
- [35] Z. Wu, J.M. McGoogan, Characteristics of and Important Lessons From the Coronavirus Disease 2019 (COVID-19) Outbreak in China: Summary of a Report of 72 314 Cases From the Chinese Center for Disease Control and Prevention, *JAMA* 323 (2020), 1239. <https://doi.org/10.1001/jama.2020.2648>.
- [36] D. Zwillinger, Fractional Differential Equations, in: *Handbook of Differential Equations*, Elsevier, 1992: pp. 258–262. <https://doi.org/10.1016/B978-0-12-784391-9.50070-1>.